HHS Public Access

Author manuscript

Biomaterials. Author manuscript; available in PMC 2015 September 16.

Published in final edited form as:

Biomaterials. 2011 April ; 32(11): 3094–3105. doi:10.1016/j.biomaterials.2010.12.054.

The impact of nanoparticle ligand density on dendritic-cell targeted vaccines

Arunima Bandyopadhyay[a], **Rebecca L. Fine**[b,c], **Stacey Demento**[a], **Linda K. Bockenstedt**[b], and **Tarek M. Fahmy**[a,d,*]

[a] Department of Biomedical Engineering, Yale University, PO Box 208260, New Haven, CT 06511, USA

[b] Department of Internal Medicine, Yale School of Medicine, USA

[c]*Williams College, Williamstown MA, USA*

[d] Department of Chemical Engineering, Yale University, PO Box 208260, New Haven, CT 06511, USA

Abstract

Dendritic-cell (DC) targeted antigen delivery systems hold promise for enhancing vaccine efficacy and delivery of therapeutics. However, it is not known how the number and density of targeting ligands on such systems may affect DC function and subsequent T cell response. We modified the surface of biodegradable nanoparticles loaded with antigen with different densities of the mAb to the DC lectin DEC-205 receptor and assessed changes in the cytokine response of DCs and T cells. DEC-205 targeted nanoparticles unexpectedly induced a differential cytokine response that depended on the density of ligands on the surface. Strikingly, nanoparticle surface density of DEC-205 mAb increased the amount of anti-inflammatory, IL-10, produced by DCs and T cells. Boosting mice with DEC-205 targeted OVA-nanoparticles after immunization with an antigen in CFA induced a similar pattern of IL-10 response. The correlation between DC production of IL-10 as a function of the density of anti-DEC-205 is shown to be due to cross-linking of the DEC-205 receptor. Cross-linking also increased DC expression of the scavenger receptor CD36, and blockade of CD36 largely abrogated the IL-10 response. Our studies highlight the importance of target ligand density in the design of vaccine delivery systems.

Keywords

Dendritic cells; C-type lectin; Nanoparticles; Cytokines; Vaccines

1. Introduction

DCs are the most potent APCs for initiating adaptive immune responses important for host defense and vaccine-induced immunity. The versatility of DCs is due to the fact that these cells are extremely adept in optimizing various endocytic and secretory pathways leading to

* Corresponding author. Department of Biomedical Engineering, Yale University, PO Box 208260, New Haven, CT 06511, USA. Tel.: +203 432 1043; fax: +203 432 0030. tarek.fahmy@yale.edu (T.M. Fahmy)..

Ag processing and presentation to cognate B and T lymphocytes [1–3]. As a consequence, promising strategies for priming T cell immunity focus on manipulating the DC response by targeting Ag delivery through specific DC surface receptors.

Pattern recognition receptors on DCs, such as TLRs and C-type lectin receptors (CLRs), sense pathogens through conserved pathogen-associated molecular patterns expressed on microorganisms. Upon ligand interaction, these receptors trigger specific cytokine responses that activate Tcell effector functions to facilitate pathogen clearance [4–10]. Steinman and his colleagues have pioneered the field of Ab-mediated targeting of Ag to DCs through several CLRs, including DEC-205 [4–6] Langerin [7] and DC-SIGN [8]. The prototypical CLR DEC-205 has been the most widely studied DC target molecule for the induction of immune responses against model and vaccine Ag [9,10]. Chimeric Abs consisting of Ag fused to the C-terminus of the heavy chain of anti-DEC-205 mAb have been shown to efficiently deliver the Ag to the late endosomal/lysosomal processing compartments for presentation by Class II MHC and CD1 molecules [5]. As DEC-205 is expressed by the CD8α+ subset of the DCs, it also helps in cross presentation of Ag. Due to the significant enhancement in both CD4 and CD8 T cell responses, DEC-205 targeted vaccination is a promising area for improving vaccine efficacy.

Micro and nanoparticles composed of biodegradable and biocompatible poly (lactide-co-glycolic acid) (PLGA) polymers are widely established platforms for controlled delivery of small molecule drugs, oligonucleotides, and protein Ags to a variety of cell types, including DCs [11–18] Several groups have demonstrated that Ag-loaded PLGA nanoparticles can induce both systemic and mucosal immunity in animals [19–23]. Indeed, several studies have demonstrated that PLGA nanoparticles have adjuvant effects comparable to those of CFA or alum, and can function as synthetic adjuvants that activate DCs to induce T cell immunity to conventional Ag [19,24,25]. Relatively little is known, however, about whether immune responses induced by nanoparticles can be enhanced by directing Ag-containing nanoparticles to DCs via CLRs. Given the multivalency of nanoparticles, (i.e. more than a few 1000 targeting Ab can be attached per particle), an additional unknown is how this multivalency might affect the DC response to Ag-containing nanoparticles to modify subsequent T cell responses.

To address this question, in this study, we examined immune responses induced by targeting OVA-containing PLGA nanoparticles to DCs. These particles were first modified with avidin into the outer layer [26] to facilitate the subsequent controlled addition of biotinylated anti-DEC-205 mAb to the particle surface. Using this construct, we analyzed the impact of multivalent DEC-205 targeted OVA-nanoparticles on the DC and T cell cytokine response in vitro and in vivo and the effect of varying the particle surface density of anti-DEC-205 mAb on the DC and T cell responses. Our studies have relevance to the design of nanoparticulate vaccines and highlight the importance of the surface density of DC target Abs on the outcome of the immune response.

2. Materials and methods

2.1. Mice

C57BL/6J (B6) mice (6–10 weeks of age, The Jackson Laboratory) were housed in a specific pathogen-free facility and animal studies were approved by the Institutional Animal Care and Use Committee at Yale University. B6 OTII TCR transgenic mice were purchased from The Jackson Laboratory and bred to produce progeny for the experiments. CD36 –/– animals were a kind gift from Dr. Daniel Goldstein's laboratory.

2.2. Isolation and purification of DCs

DCs were generated from bone marrow cells collected from the femurs and tibias of mice according to established techniques [55]. After RBC lysis with ammonium chloride (Sigma), the remaining bone marrow cells were cultured for 6d in complete RPMI medium (RPMI supplemented with 10% FBS, 1% L-glutamine, 1% HEPES buffer, non-essential amino acids, 0.1% 2-ME, 50 μg/ml streptomycin, 50 IU/ml penicillin) and 20 ng/ml recombinant murine GM-CSF. At the end of the incubation, nonadherent cells were discarded and adherent cells were dislodged and purified by positive selection using a CD11c EasySep column (Stem cell Technologies). Flow cytometry confirmed that >90% of the cells were $CD11c^{hi\ i}$ and $CD80^{lo}$, $CD86^{lo}$, and $IA^{b(lo)}$. OVA-specific OTII Tg T cells were purified from mouse splenocytes after RBC lysis using the mouse CD4+ T cell enrichment kit (Stem cell Technologies).

2.3. Synthesis of nanoparticles

PLGA 50/50 with an average molecular weight of 80 kd was obtained from Durect Corporation (Cupertino, CA).Nanoparticles that encapsulated OVA and were functionalized with avidin were manufactured using a modified double emulsion of water–oil–water technique [26].

2.4. Characterization of nanoparticles

The lyophilized nanoparticles were visualized by scanning electron microscopy. The amount of OVA encapsulated in the nanoparticles was quantified using the Micro BCA Protein Assay (Pierce) after dissolving the particles in 0.05 N NaOH with 1% SDS. The amount of avidin per mg of the particles was quantified using the Micro BCA Protein assay. Particle sizes were also measured by dynamic light scattering using a Zeta Plus Particle Sizer (Brookhaven Instruments Corporation). The mean diameters of the nanoparticles with and without Ab were reported from the multimodal size distribution that was obtained using the Zeta Plus Particle Sizing software v2.27 (Brookhaven Instruments Corp).

2.5. Ligand coupling to the particle surface

Biotinylated anti-mouse DEC-205 mAb (clone NLDC 145) (BACHEM, CA) was added at various concentrations between 0 and 25 μg/ml to a 5 mg/ml solution of PLGA particles in PBS and rotated for 20–30 min at room temperature. The particles were then centrifuged at 13,000 rpm for 5 min and the supernatant removed to measure the amount of unbound Ab remaining using the Micro BCA Protein Assay Kit. All mAb was bound as no protein was

detected in the particle supernatant (data not shown). The release of Ag from the particles in aqueous solution was not altered by the addition of anti-DEC-205 mAb to the particle surface (data not shown).

2.6. Flow cytometry assessment of particle internalization

DCs were aliquoted at 10^6 cells/ml in RPMI media + 10% FBS supplemented with L-glutamine, MEM non-essential amino acids, HEPES buffer, gentamicin, and β-mercaptoethanol in a 24 well plate for 1 h to allow adherence. The DCs were then incubated with 100 μg/ml of coumarin-6 encapsulated nanoparticles for 1, 4 or 8 h. At the indicated times, the cells were washed twice with PBS + 1% FBS. The cells were then labeled with APC-conjugated CD11c mAb (eBioscience) for 30 min at 4 °C. After staining, the cells were washed with PBS + 1% FBS and then fixed with 4% paraformaldehyde prior to flow cytometric analysis using a FACS Calibur system (BD). Differences in mean fluorescence intensity for coumarin-6 were assessed by the Student's *t* test using GraphPad, Prism, version 4.0b software.

2.7. Assessment of particle internalization by confocal microscopy

DCs were plated on alcian blue coated glass cover slips at a seeding density of 2×10^5 cells per cover slip for 1 h at 37 °C to allow adherence. After rinsing to remove nonadherent cells, cells were incubated with 100 μg/ml of coumarin-containing nanoparticles for 1, 4 or 8 h at 37 °C. At the end of the incubation period, the media was removed and cells were washed once with PBS + 1% FBS and then fixed in 4% paraformaldehyde. Cells were permeabilized using 0.1% triton-X 100 in PBS and then stained with a 1:200 dilution of Alexa 548-phalloidin and 1:500 dilution ToPro-3 (Molecular Probes) to delineate the cytoskeleton and nucleus, respectively. Cells were visualized under Zeiss confocal microscope (LSM 510) using wavelengths 488, 568 and 633 nm.

2.8. Stimulation of DCs and T cells

DCs were aliquoted into 96-well microtiter plates at 2×10^5 cells/well and allowed to adhere overnight. Nanoparticles (200 μg/ml) were added to triplicate wells of DCs in 100 μl total volume and the cultures were incubated for 4 or 8 h in a 37 °C humidified CO_2 incubator. Wells were then washed twice to remove uningested particles before adding fresh media. After 24 h, supernatants were harvested and assayed for IL-12 and IL-10 using cytokine-specific ELISA (BD Pharmingen).

For measurement of T cell responses, DCs that had been pulsed with nanoparticles as described above were washed extensively to remove uningested particles. Purified naïve OTII Tg T cells were added at 2:1 ratio (T:DC) and incubated for 72 h in a 37 °C humidified CO_2 incubator. At the end of this period, supernatants were harvested and the amount of IL-2, IL-5, IL-10 and IFNγ was quantified using cytokine-specific ELISA (BD Pharmingen).

In some assays, DCs were stimulated with soluble OVA in combination with anti-DEC-205 mAb, avidin-biotinylated anti-DEC-205 mAb complexes, or avidin with anti-DEC-205 mAb. Additionally, DCs were stimulated with a soluble fusion protein containing OVA and

the heavy chain of anti-DEC-205 mAb (s-OVA-DEC-205, a kind gift of Dr. Ira Mellman, Genentech). After Fc receptor blockade, DCs were stimulated with the indicated Ag preparations containing 0, 5, 10 or 25 μg/ml anti-DEC-205 mAb. Cytokines elicited were measured as described above.

2.9. Measurement of CD36 and DC activation markers by flow cytometry

DCs were aliquoted at 1×10^6 cells/ml complete RPMI (1 ml/well) in a 24 well plate and allowed to adhere for 1 h. The DCs were incubated with 200 μg/ml of the different concentrations of targeted or non-targeted nanoparticles that delivered equivalent amounts of anti-DEC-205 mAb. After 8 h of incubation, wells were washed to remove uningested stimuli and fresh media was added to cells. After 24, 48 and 72 h, aliquots of cells were stained with PE-conjugated anti-mouse CD36 mAb (eBioscience) (1:200 dilution) or an isotype control, FITC-conjugated anti-mouse CD80 (BD Bioscience) mAb (1:100 dilution), PE-conjugated anti-mouse CD86 mAB (1:200 dilution) (BD Bioscience) or FITC-conjugated anti-mouse IA^b (1:150 dilution) (eBioscience). In some cases, the cells were then washed twice with PBS supplemented with 1% FBS, fixed with formaldehyde and the fluorescence intensity of FITC staining was measured by flow cytometry using a FACS Calibur.

2.10. Measurement of DC and T cell responses after CD36 blockade and in CD36 –/– animals

DCs were aliquoted at 1×10^6 ells/ml complete RPMI (1 ml/well) in a 24 well plate and allowed to adhere for 1 h. Cells in duplicate wells were then treated with 20 μg/ml anti-CD36 mAb (FA6152, Abcam), and anti-mouse IgG1 (isotype control) or no Ab. After 1 h, 200 μg/ml OVA-nanoparticles coated with the indicated concentrations of anti-DEC-205 mAb were added to duplicate wells. After 8 h incubation at 37 °C, uningested particles were washed off and either fresh media was added to cells for assessment of DC responses or media containing purified CD4+ OTII Tg T cells at a T:DC ratio of 2:1 was added to assess T cell responses. Supernatants were harvested from DC cultures after 24 h and from T cell cultures after 72 h incubation at 37 °C. Cytokines were analyzed using cytokine-specific ELISA as described above (BD Pharmingen). Similar experiments were repeated with CD14 +/– and CD36 –/– animals on a C57/BL6 background and the DC and T cell cytokine responses were compared with the wild type animals.

2.11. Mice immunization

Groups of 4 mice were immunized by i.p. injection of 100 μg OVA emulsified in CFA (200 μl total volume, Pierce) or sham immunized with 200 μl PBS. One wk later, groups of mice were boosted by i.p injection of 300 μl PBS containing 2 mg OVA-nanoparticles (40 μg OVA) that had been surface modified with 0, 0.5, 1 or 5 μg/ml anti-DEC-205 mAb. One week after secondary immunization, mice were sacrificed and splenocytes harvested. Whole splenocytes in complete RPMI were aliquoted at 2×10^5 cells/well into 96 well round bottom plates and stimulated with 200 μg/ml OVA for 72 h, after which cell free supernatants were collected and analyzed for IL-2, IL-5, IL-10 and IFNγ by ELISA (BD Pharmingen). In another set of in vivo experiments, groups of 4 mice were immunized i.p. with 300 μl PBS containing 2 mg OVA-nanoparticles (30 μg OVA) surface modified with 0,

0.5 or 5 μg/ml anti-DEC-205 mAb. Mice were also immunized with similar concentrations of OVA (30 μg) in CFA and OVA (30 μg) in Alhydrogel, prepared by mixing OVA and Alhydrogel (1 μl/μg protein). Serum isolated at week 2 and analyzed for OVA specific titers of total IgG, IgG1, IgG2b, and IgG2c by ELISA. Blank nanoparticles containing no OVA were used as the negative controls. Experiments were repeated two times and the statistical differences between controls and experimental groups were determined using Student *t* test.

2.12. Ab titer analysis

Blood samples were retro orbitally collected from all animals and were allowed to clot at 4 °C overnight. Samples were then centrifuged at 3000 rpm for 10 min and serum stored at –80 °C. High binding plates were coated with 50 μg OVA (Sigma grade V) in PBS and incubated overnight at 4 °C. Serial dilutions of serum in blocking buffer was performed and plates were incubated with these after blocking with blocking buffer (PBS + 5% BSA [Sigma–Aldrich] + 0.1% Tween 20 [Sigma–Aldrich]). Plates were washed thrice and HRP-conjugated goat anti-mouse IgG1, IgG2c, IgG2b (Invitrogen) and total IgG (Jackson ImmunoResearch Laboratories, West Grove, PA) were added in blocking buffer at a 1:2000 dilution. Plates were washed after 1 h and developed using tetramethylbenzidine substrate (Kirkegaard & Perry Laboratories, Gaithersburg, MD). 1 N HCl was used to stop the reaction and absorbance was measured by a spectrophotometer at 450 nm. The inverse dilution at which absorbance equaled that of the control was calculated as titer. The control samples were mice receiving no Ag plus 2 SD. After a log transformation of values, the linear regression of dilution versus Ab curve was calculated.

3. Results

3.1. Particle preparation and characterizatoin

Previously we developed a strategy for surface modification of PLGA particles by introducing functionally active avidin coupled to palmitic acid during the emulsion preparation of the particles [26]. We demonstrated that functionalizing PLGA with avidin-palmitic acid facilitated incorporation of avidin at high density on the surface. The fatty acid anchoring the avidin preferentially associated with the hydrophobic PLGA matrix while the hydrophilic avidin partitioned to the surface. These particles can then be further surface modified by the addition of biotinylated molecules that bind avidin with high affinity. This system leads to prolonged presentation of the biotinylated molecules over the course of several weeks while release of proteins from the PLGA matrix is unhindered [13,18,27].

Ova-containing PLGA nanoparticles functionalized with avidin-palmitic acid were surface modified with varying amounts of biotinylated anti-DEC-205 mAb (Fig. 1A, B). In all the experiments reported here we have used these nanoparticles with avidin-palmitate with or without different concentrations of targeting antibody. Functionalized, non-targeted nanoparticles and DEC-205 targeted nanoparticles were characterized by dynamic light scattering to ascertain whether the surface modification with different densities of DEC-205 mAb affected the mean diameter of the particles. No significant increase in the mean diameter between the non-targeted and the targeted particles was detected, even with the highest density of anti-DEC-205 mAb, which remained well within the nanoparticle size

range of 200e250 nm (Fig. 1C). Release of Ag from the particles was also similar (data not shown).

3.2. Nanoparticle induction of DC and T cell cytokine responses

To determine the effects of targeting nanoparticles to DEC-205 on DCs, we measured cytokines from the supernatants of DCs 24 h after an 8 h exposure to DEC-205 targeted (white bars), control IgG coated OVA-nanoparticles (stippled bars) or non-targeted nanoparticles without Ag (black bars). DCs exposed to any preparation of OVA-nanoparticles produced high concentrations of IL-12 (Fig. 2A, white and stippled bars). Unexpectedly, we found that DCs exposed to DEC-205 targeted nanoparticles also produced IL-10, with the amount secreted dependent on the density of anti-DEC-205 mAb on the particle surface (Fig. 2B, white bars). Nanoparticle-stimulated DCs co-cultured with OVA-specific CD4+ OTII Tg cells for 72 h showed differential cytokine production that also was dependent upon the density of anti-DEC-205 mAb on the nanoparticle surface. Whereas IFNγ and IL-2 production by T cells was similar with IgG coated OVA-nanoparticles (Fig. 2C, D, stippled bars) and DEC-205 targeted OVA-nanoparticles (Fig. 2C, 2D, white bars), IL-10 production was only seen in supernatants of T cells stimulated with DCs that had been exposed to OVA-nanoparticles modified with anti-DEC-205 mAb (Fig. 2E, white bars). IL-5 was also produced by T cells stimulated with DCs primed with either targeted or non-targeted nanoparticles, but the greatest amount was seen with OVA-nanoparticles coated with the highest amount of anti-DEC-205 mAb (Fig. 2F). The amount of IL-10 and IL-5 produced by T cells was dependent on the amount of anti-DEC-205 mAb on the particle surfaces. DCs stimulated with blank nanoparticles containing no Ag but coated with DEC-205 produced negligible levels of cytokines compared to the ones containing OVA as Ag under these conditions. It has been shown in other studies that PLGA nanoparticles encapsulating peptide enhances the stimulatory properties of DCs when compared to blank nanoparticles containing no Ag [28]. Similar patterns of cytokines were seen when DCs were exposed to nanoparticles for 4 h (data not shown).

3.3. DC and T cell cytokine responses by soluble fusion protein DEC-205-OVA

Differential IL-10 production by DCs has not been previously observed with exposure to chimeric proteins containing both anti-DEC-205 mAb and Ag. To ascertain if the observed differences in IL-10 production by DCs and Tcells could be recapitulated when Ag is introduced using anti-DEC-205 mAb, we used a soluble fusion protein containing light and heavy chains of mouse anti-DEC-205 mAb coupled to OVA (s-OVA-DEC-205 mAb). DCs were stimulated for 8 h with s-OVA-DEC-205 mAb containing 5–25 μg/ml anti-DEC-205 mAb to approximate the range of concentrations of anti-DEC-205 mAb on the OVA-nanoparticles. We found that Tcells stimulated with DCs primed with s-OVA-DEC-205 mAb produced IFNγ and IL-2 in amounts comparable to stimulation with DEC-205 targeted OVA-nanoparticles (Fig. 2C, D, gray bars). However, there was minimal IL-10 and IL-5 elicited by the s-OVA-DEC-205 mAb construct in comparison to nanoparticles having anti-DEC-205 mAb on their surfaces (Fig. 2E, F, gray bars), consistent with the low level of induction of IL-10 by DCs primed with the fusion protein.

3.4. Nanoparticle induction of in vivo secondary immune responses

In order to determine whether our in vitro observations could be reproduced in vivo, we examined the T cell cytokine profiles induced when DEC-205 targeted OVA-nanoparticles were used to boost the primary immune response to OVA in CFA. The adjuvant CFA is known to prime for Th1 responses to Ag, and our aim was to determine whether the surface modified nanoparticles could modify this response. We found that boosting mice with either non-targeted or DEC-205 targeted OVA-nanoparticles could augment IL-2 and IFNγ production in comparison to primary immunization with OVA in CFA alone (Fig. 3A, B). Consistent with our observed in vitro studies, exposure to DEC-205 targeted particles also resulted in T cell production of IL-10 and IL-5, with more cytokine produced correlating to the greatest density of anti-DEC-205 mAb on the particle surfaces (Fig. 3C, D).

3.5. Nanoparticle internalization

To determine whether differential IL-10 production was a result of differential uptake mediated by the surface density of the antibody target, we measured particle internalization as a function of time. Nanoparticles were synthesized encapsulating the dye Coumarin-6 and were surface modified with avidin. We chose this dye because it is known to associate tightly with the nanoparticle polymer core and does not degrade or release with time [29]. Purified DCs were exposed to 150 μg/ml of non-targeted or targeted nanoparticles, and then harvested at different time points for analysis of particle uptake by flow cytometry. DCs exposed to non-targeted particles that were held at 4 °C (Fig. 4B) revealed no significant uptake relative to unstained cells (Fig. 4A) or DCs incubated at 37 °C (Fig. 4C, D, and E). At 1 h, there was a modest difference in the amount of non-targeted particle uptake in comparison to targeted particle uptake as assessed by cell fluorescence (Fig. 4C). At 4 h and 8 h, however, the internalization of the non-targeted and targeted nanoparticles was comparable (Fig. 4D, E), indicating that differences in particle uptake could not explain the differential cytokine induction by DCs exposed to targeted nanoparticles for a similar duration.

The internalization of non-targeted and surface modified nanoparticles was also assessed using confocal microscopy (Fig. 5). DCs were incubated with the different surface modified and non-targeted dye-labeled nanoparticles for 1 h, 4 h and 8 h, then washed, permeabilized, and stained with the cytoskeletal marker Alexa 546 Phalloidin and the nuclear stain ToPro-3. The results were consistent with flow cytometry data and showed that there were negligible differences in uptake of non-targeted and targeted particles at the time points analyzed (Fig. 5A, B and C). No significant uptake was detected when DCs were exposed to particles and kept at 4 °C (Fig. 5D).

3.6. DEC-205 cross-linking on DC surfaces by soluble complexes of avidin and biotin anti-DEC-205

Given the fact that internalization of particles was independent of the density of targeting ligand, we next asked if the observed differential IL-10 responses were associated with a cell surface binding phenomenon that was dependent on the density of the targeting ligand. To address this question, we incubated DCs with soluble anti-DEC-205 mAb or a multivalent form produced by complexing biotinylated anti-DEC-205 mAb with avidin. As a control,

DCs were also stimulated with avidin and soluble, non-biotinylated anti-DEC-205 mAb. All DC cultures were simultaneously exposed to OVA. We observed that indeed multimeric complexes of avidin-biotinylated anti-DEC-205 mAb produced concentrations of IL-10 that depended on the amount of biotinylated anti-DEC-205 mAb (Fig. 6A, white bars). The amount of IL-10 elicited was similar to the dose-dependency seen with increasing anti-DEC-205 Ab on the surface of the nanoparticles (Fig. 6A versus Fig. 2E). Minimal IL-10 was detected when DCs were stimulated with OVA, avidin and unbiotinylated anti-DEC-205 mAb (Fig. 6A, gray bars) or OVA plus biotinylated anti-DEC-205 mAbwithout avidin (Fig. 6A, black bars). Tcell production of IL-10 was dependent on the concentration of OVA in DC cultures, with lower concentrations of OVA eliciting less IL-10 (data not shown). As further confirmation of our findings, DCs were stimulated with soluble OVA and anti-DEC-205 mAb coated nanoparticles that contained no Ag or with soluble anti-DEC-205 mAb and OVA encapsulated nanoparticles that contained no avidin (or surface modification with anti-DEC-205 mAb) (Fig. 6B). IL-10 was produced by T cells only when the DCs had been exposed to Ag and anti-DEC-205 mAb coated nanoparticles and responses were similar to those observed with OVA encapsulated in targeted nanoparticles. Taken together, these findings suggest that cross-linking DEC-205 on the DC surface during Ag uptake and presentation is required for DCs to induce T cells to produce an anti-inflammatory response.

3.7. CD36 expression after nanoparticle treatment

In related studies, we found using DC microarray analysis that one of the genes most highly induced by DEC-205 targeted nanoparticles in comparison to non-targeted nanoparticles was the scavenger receptor CD36 (manuscript in preparation). This molecule is a receptor for thrombospondin I involved in the uptake of apoptotic cells, bacteria and fungal pathogens [30–32]. Induction of CD36 expression was assessed by flow cytometric analysis of DCs stimulated with s-OVA-DEC-205 mAb, non-targeted nanoparticles, or DEC-205 targeted nanoparticles. The surface expression of CD36 increased only with nanoparticles that were surface modified with anti-DEC-205 mAb, and the level of expression correlated with the amount of anti-DEC-205mAb on the surface (Fig. 7A,B, blueline). Concentrations of the s-OVA-DEC-205 mAb conjugate equivalent to those expressed on the targeted nanoparticles did not increase surface expression of CD36 on DCs to the same extent (Table 1). These results clearly associate CD36 upregulation with DC exposure to nanoparticles with high density anti-DEC-205 mAb. In contrast, differences in the surface modifications of the nanoparticles did not cause any discernible difference in upregulation of the DCactivation marker IA^b (Fig. 7E) or T cell costimulatory molecules CD80 (Fig. 7C) and CD86 (Fig. 7D).

3.8. DC and T cell cytokine responses after blockade or deletion of CD36

Recently, it has been shown that CD36 upregulation is associated with anti-inflammatory effects and increased secretion of IL-10 [33]. To ascertain this association within the context of administering our particles, we performed a blockade experiment with an Ab that blocks the thrombospondin-1 binding site of CD36 (FA6152, Abcam). Our results showed that blocking the thrombospondin-1 binding site of CD36 significantly reduced the IL-10 responses from both the DCs and the T cells when treated with the high anti-DEC-205

coated nanoparticles (Fig. 8). To confirm our findings further, we used CD36 –/– mice to study the effect of these different surface modified nanoparticles. Our results show that DCs and T cells deficient in the CD36 gene showed a considerable decrease in IL-10 production when compared to the wild type animals. This highlights the involvement of CD36 in cytokine production from DCs and Tcells when treated with non-targeted as well as targeted particles. Hence in this case the production of IL-10 is partially dependent on the upregulation of the scavenger receptor CD36.

3.9. Ag specific Ab titers

Mice were immunized with the different surface modified nanoparticles (with 0, 0.5 or 5 μg/ml) anti-DEC-205 and OVA/CFA as well as OVA/Alhydrogel. After 2 weeks, serum was isolated from these animals and OVA specific Ab titers were measured. The total OVA specific IgG titers were highest for CFA/OVA and Alhydrogel/OVA. The different surface modified nanoparticles also showed an enhanced Ab response as revealed by the high OVA specific IgG titers.

These nanoparticles elicited similar total IgG responses and IgG2c and IgG2b responses (Fig. 9). This observation further confirms that the different surface modifications of these particles produce similar levels of Th1 cytokines. The IgG2c and IgG2b responses (Th1 biased response) were highest for CFA/OVA as expected. Interestingly, the high anti-DEC-205 coated nanoparticles elicited a higher IgG1 response (Th2 biased response) compared to the low anti-DEC-205 coated nanoparticles or the untargeted ones. Alum showed the highest IgG1 response as expected. Thus these studies show that particles modified with high anti-DEC-205 show a differential Th2 response when compared to the other particles.

4. Discussion

Nanoparticle technology has been shown to provide versatile and effective platforms for the delivery of vaccine Ag. The particulate nature of these systems permits their rapid internalization by DCs and their composition can provide adjuvant properties required for immunogenicity without the need for conventional adjuvants [17,34,35]. The targeting of vaccine Ag, via modified liposomes or surface modified nanoparticles, to pattern recognition receptors on DCs has improved upon the immunogenicity of Ag delivered in this fashion [36–40]. Ag encapsulated in biomaterials and targeted to APCs are protected from enzymatic degradation, and processed and presented to T lymphocytes after their delivery to the APCs [41–43].

Here we show how surface modification of Ag-loaded nanoparticles to direct them to DCs affects the outcome of an immune response. OVA-nanoparticles conjugated with mAb to the C-type lectin receptor DEC-205 induced DCs to produce IL-10, with levels correlating with the amount of anti-DEC-205 mAb on the particle surface. Notably, production of IL-10 was not associated with reduction in IL-12, and T cells primed with these DCs in vitro produced IFNγ as well as IL-10 and IL-5. The in vitro experiments were repeated with DCs derived from MyD88 knock out animals (data not shown) and similar results were obtained. Thus LPS or endotoxin contamination was not responsible for the production of these cytokines.

When used to boost mice previously immunized with OVA and CFA, a Th1-inducing adjuvant, DEC-205 targeted OVA-nanoparticles not only enhanced the T cell production of IFNγ, but also induced T cell production of IL-10 and IL-5. Boosting T cell production of IFNγ was not unexpected as non-targeted PLGA nanoparticles containing OVA are capable of eliciting a Th1 response in vivo. However, only the production of IL-10 and IL-5 was influenced by the density of anti-DEC-205 mAb on the particle surface, as observed both in vitro and in vivo. These findings suggest that the effects of the nanoparticles on the DC involve two pathways: a pathway through which PLGA nanoparticles induced production of IL-12 and a second DEC-205-associated pathway that also elicited the production of IL-10. In another in vivo experiment, mice were immunized with the high and low concentrations of anti-DEC-205 mAb on the surface of the nanoparticles as well as non-targeted ones. Controls were OVA adsorbed in CFA and OVA in alum. Serum from these animals were isolated at week 2 and analyzed for circulating Ag specific Ab. The OVA specific IgG1 Abs were slightly higher for the mice receiving high anti-DEC-205 coated nanoparticles, compared to the untargeted or the low anti-DEC-205 coated particles, confirming that the Th2 biased response is higher with the high anti-DEC-205 particles. There was no difference in the total OVA specific IgG responses as well as the IgG2b and IgG2c responses for all the groups of mice treated with nanoparticles. The Th1 specific cytokines were unaltered for these particles based on all our observations.

Several studies have demonstrated that targeting Ag to DCs via CLRs improves receptor-mediated endocytosis and Ag presentation. For example, using mannosylated liposomes that bind the mannose receptor on DCs, Epsuelas et al. showed that human DCs endocytosed the mannosylated liposomes more readily than non-targeted liposomes [44], with liposomes containing di- and tetraantennary mannosyl lipid derivatives equally effective at Ag delivery. The CLR DEC-205 has an acidic amino acid sequence that targets ligands to late endosomes where MHC-II acquires Ag [45]. Thus targeting this receptor delivers Ag to MHC-II Ag presentation to a great extent. Kwon et al. used pH responsive microparticles surface conjugated with anti-DEC-205 mAb to demonstrate that targeting DEC-205 enhances particle uptake and Ag presentation. In vivo and ex vivo studies with anti-DEC-205 conjugated microparticles showed that these particles were more efficiently internalized by DCs, and migration of DCs carrying these particles to the lymph nodes produced enhanced cellular immunity [46].

Our study is the first to examine the effects of the density of the DC targeting ligand on the outcome of the immune response to Ag-loaded nanoparticles. Given the particulate, multivalent nature of nanoparticle systems, which are capable of presenting hundreds or thousands of targeting groups per particle, simply attaching a DC specific ligand to the particle surface can lead to striking results as demonstrated in this work. Unlike studies with anti-DEC-205 mAb conjugated microparticles, targeted nanoparticles were more efficiently ingested than non-targeted particles if exposure was limited (e.g. 1 h), making this mechanism an unlikely explanation for the unique cytokine profile induced by DCs exposed for up to 8 h to DEC-205 targeted nanoparticles.

Similar dose dependent enhancement of IL-10 was observed with increasing densities of mannosamine on the surface of these particles when mannose receptor which is both a CLR

and a scavenger receptor, was targeted (data not shown). Recent work by Chieppa et al. has shown that cross-linking mannose receptors on the surface of DCs lead to an anti-inflammatory program [47]. Monocyte-derived DCs in which the mannose receptor was cross-linked using a mannose receptor-specific mAb PAM-1 were unable to produce any IL-12 but instead secreted IL-10 and other tolerogenic cytokines and chemokines. This cytokine profile was distinct from that produced by DCs matured by exposure to LPS. Their work showed that cross-linking mannose receptors on myeloid DCs by particular Abs or ligands produce anti-inflammatory and tolerogenic cytokines, thus preventing Th1 responses. In our study, however, we found that DEC-205 targeted OVA-nanoparticles primed DCs to produce IL-12 and IL-10, which elicited IFNγ, IL-10 and IL-5 from responding T cells. Little is known about DEC-205 in terms of its natural ligands, signaling motif or the signaling proteins involved. Nanoparticles modified with varying densities of ligand on their surface potentially mimic multivalent ligands and are capable of cross-linking surface receptors. Multivalent ligands can crosslink the membrane receptors more efficiently to regulate signaling processes [48–50]. It is possible that substantial cross-linking of the DEC-205 receptors occurred due to the multivalency induced by incorporating avidin in the nanoparticle for binding biotinylated anti-DEC-205 mAb. When we mimicked the multivalent nature of the anti-DEC-205 mAb coated nanoparticles by forming large soluble complexes of equivalent concentrations of biotinylated anti-DEC-205 mAb and avidin, we observed similar dose dependent IL-10 production. Thus different degrees of receptor cross-linking in this case has broadened DC and T cell cytokine responses.

We found that targeting nanoparticles to DEC-205 increased surface expression of the scavenger receptor CD36 on DCs. This receptor is present on a wide variety of cells, including platelets, mononuclear phagocytes, adipocytes, hepatocytes, and myocytes [51]. CD36 is involved in cellular adhesion and lipid metabolism [52] as well as innate immune responses to oxidized LDL, β-amyloid and Ag of *Plasmodium falciparum* [30,31,53] Immunosuppressive effects of apoptotic cells or agents that cause an increase in CD36 expression on binding to this receptor have been shown to lead to IL-10 production. Chung et al. showed that apoptotic cell uptake by macrophages leads to IL-10 production, a response that is at least partially dependent on CD36, as CD36 deficient macrophages exposed to apoptotic cells produced much less IL-10 [33]. Our results show that targeting nanoparticles to DEC-205 increases DC expression of CD36, and mAb blockade of the TSP-1 binding site on CD36 also diminishes IL-10 production by DCs exposed to DEC-205 targeted OVA-nanoparticles. These results were further confirmed using mice deficient in CD36 gene. This finding implicates CD36 in the induction of an anti-inflammatory cytokine program, possibly because the DEC-205 targeted nanoparticles are mimicking apoptotic cells. A recent study showed that DEC-205 can act as a receptor that can recognize dying cells and apoptotic cells, although the exact mechanism underlying recognition of dead cells is not known [32]. CD36 has recently been shown to be an excellent receptor for APC targeting to enhance immunity. Tagliani et al. have observed a 300-fold enhancement in the delivery of peptides to the classical MHC class II and the cross-presentation pathways by CD36-mediated endocytosis of soluble Ags [54].

5. Conclusions

In summary, we have identified a phenomenon whereby DEC-205 targeted Ag-loaded nanoparticles induce DCs and T cells to produce Th2 associated cytokines without impeding DC priming of a Th1 response. Multivalent cross-linking of the DEC-205 receptor on the DC is required for the response, and is associated with the upregulation of the scavenger receptor CD36 on the DC. Additional studies are needed to determine whether unique subsets of DCs and/or T cells are involved in production of these cytokines. Our findings highlight the importance of ligand density in the outcome of an immune response to DC targeted nanoparticle based vaccine delivery systems.

Acknowledgments

The authors thank Michael Look and Feng Qian for excellent technical support and, Lelia Delamarre, Ira Mellman (Genentech Inc.) and Jason Criscione for helpful comments regarding the manuscript. This work was supported by NSF NIRT grant #CTS-0609326 to TMF, National Research Service Award (NRSA) postdoctoral fellowship (5T32 HL007974-08) to AB and the Jockers Award to LKB.

Appendix

Figures with essential color discrimination. Certain figures in this article, particularly Figs. 1, 5 and 7 are difficult to interpret in black and white. The full color images can be found in the online version, at doi:10.1016/j.biomaterials.2010.12.054.

The following abbreviations were used

PLGA	poly (lactic co-glycolic acid)
TLR	Toll-like receptor
CLR	C-type lectin receptor
Ag	antigen
s-OVA-DEC-205 mAb	soluble fusion protein containing light and heavy chains of mouse anti-DEC-205 mAb coupled to OVA

References

1. Banchereau J, Steinman RM. Dendritic cells and the control of immunity. Nature. 1998; 39:245–52. [PubMed: 9521319]
2. Steinman RM, Hemmi H. Dendritic cells: translating innate to adaptive immunity. Microbiol Immunol. 2006; 311:17–58.
3. Steinman RM, Banchereau J. Taking dendritic cells into medicine. Nature. 2007; 449:419–26. [PubMed: 17898760]
4. Nchinda G, Kuroiwa J, Oks M, Trumpfheller C, Park CG, Huang Y, et al. The efficacy of DNA vaccination is enhanced in mice by targeting the encoded protein to dendritic cells. J Clin Invest. 2008; 118:1427–36. [PubMed: 18324335]
5. Bonifaz LC, Bonnyay DP, Charalambous A, Darguste DI, Fujii S, Soares H, et al. In vivo targeting of antigens to maturing dendritic cells via the DEC-205 receptor improves T cell vaccination. J Exp Med. 2004; 199:815–24. [PubMed: 15024047]

6. Bozzacco L, Trumpfheller C, Siegal FP, Mehandru S, Markowitz M, Carrington M, et al. DEC-205 receptor on dendritic cells mediates presentation of HIV gag protein to CD8+ T cells in a spectrum of human MHC I haplotypes. Proc Natl Acad Sci USA. 2007; 104:1289–94. [PubMed: 17229838]
7. Idoyaga J, Cheong C, Suda N, Suda J, Kim Y, Lee H, et al. Cutting edge: langerin/CD207 receptor on dendritic cells mediates efficient antigen presentation on MHC I and II products in vivo. J Immunol. 2008; 180:3647–50. [PubMed: 18322168]
8. Singh SK, Stephani J, Schaefer M, Kalay H, García-Vallejo JJ, den Haan J, et al. Targeting glycan modified OVA to murine DC-SIGN transgenic dendritic cells enhances MHC class I and II presentation. Mol Immunol. 2009; 47:164–74. [PubMed: 19818504]
9. Trumpfheller C, Finke JS, López CB, Moran TM, Moltedo B, Soares H, et al. Intensified and protective CD4+ T cell immunity in mice with anti-dendritic cell HIV gag fusion antibody vaccine. J Exp Med. 2006; 203:607–17. [PubMed: 16505141]
10. Gurer C, Strowig T, Brilot F, Pack M, Trumpfheller C, Arrey F, et al. Targeting the nuclear antigen 1 of Epstein-Barr virus to the human endocytic receptor DEC-205 stimulates protective T-cell responses. Blood. 2008; 112:1231–9. [PubMed: 18519810]
11. Bala I, Hariharan S, Kumar MN. PLGA nanoparticles in drug delivery: the state of the art. Crit Rev Ther Drug Carrier Syst. 2004; 21:387–422. [PubMed: 15719481]
12. Walter E, Dreher D, Kok M, Thiele L, Kiama SG, Gehr P, et al. Hydrophilic poly(dl-lactide-co-glycolide) microspheres for the delivery of DNA to human-derived macrophages and dendritic cells. J Control Release. 2001; 76:149–68. [PubMed: 11532321]
13. Park J, Fong PM, Lu J, Russell KS, Booth CJ, Saltzman WM, et al. PEGylated PLGA nanoparticles for the improved delivery of doxorubicin. Nanomedicine. 2009; 4:410–8. [PubMed: 19341815]
14. Demento SL, Bonafé N, Cui W, Kaech SM, Caplan MJ, Fikrig E, et al. TLR9-targeted biodegradable nanoparticles as immunization vectors protect against West Nile encephalitis. J Immunol. 2010; 185:2989–97. [PubMed: 20660705]
15. Xiang SD, Cordella S, Ho J, Apostolopoulos V, Plebanski M. Delivery of DNA vaccines: an overview on the use of biodegradable polymeric and magnetic nanoparticles. Wiley Interdiscip Rev Nanomed Nanobiotechnol. 2010; 3:205–18. [PubMed: 20391461]
16. Kaiser-Schulz G, Heit A, Quintanilla-Martinez L, Hammerschmidt F, Hess S, Jennen L, et al. Polylactide-coglycolide microspheres co-encapsulating recombinant tandem prion protein with CpG-oligonucleotide break self-tolerance to prion protein in wild-type mice and induce CD4 and CD8 T cell responses. J Immunol. 2007; 179:2797–807. [PubMed: 17709493]
17. Fahmy TM, Demento SL, Caplan MJ, Mellman I, Saltzman WM. Design opportunities for actively targeted nanoparticle vaccines. Nanomedicine. 2008; 3:343–55. [PubMed: 18510429]
18. Demento SL, Eisenbarth SC, Foellmer HG, Platt C, Caplan MJ, Saltzman WM, et al. Inflammasome-activating nanoparticles as modular systems for optimizing vaccine efficacy. Vaccine. 2009; 27:3013–21. [PubMed: 19428913]
19. Jaganathan KS, Vyas SP. Strong systemic and mucosal immune responses to surface-modified PLGA microspheres containing recombinant hepatitis B antigen administered intranasally. Vaccine. 2006; 24:4201–11. [PubMed: 16446012]
20. Gupta PN, Khatri K, Goyal A, Mishra K, Vyas SP. M-cell targeted biodegradable PLGA nanoparticles for oral immunization against hepatitis B. J Drug Target. 2007; 15:701–13. [PubMed: 18041638]
21. Feng L, Qi XR, Zhou XJ, Maitani Y, Wang SC, Jiang Y, et al. Pharmaceutical and immunological evaluation of a single-dose hepatitis B vaccine using PLGA microspheres. J Control Release. 2006; 112:35–42. [PubMed: 16516999]
22. Jaganathan KS, Singh P, Prabakaran D, Mishra V, Vyas SP. Development of a single-dose stabilized poly(d, l-lactic-co-glycolic acid) microspheres-based vaccine against hepatitis B. J Pharm Pharmacol. 2004; 56:1243–50. [PubMed: 15482638]
23. Yuba E, Kojima C, Harada A, Tana A, Watarai S, Kono K. pH-sensitive fusogenic polymer-modified liposomes as a carrier of antigenic proteins for activation of cellular immunity. Biomaterials. 2010; 31:943–51. [PubMed: 19850335]

24. Xu L, Kurtz SL, Liu J, Braunstein M, McMurray DN, Hickey AJ. Poly (lactide-co-glycolide) microspheres in respirable sizes enhance an in vitro T cell response to recombinant *Mycobacterium tuberculosis* antigen 85B. J Pharm Res. 2007; 24:1834–43.
25. Gutierro I, Hernández RM, Igartua M, Gascón AR, Pedraz JL. Size dependent immune response after subcutaneous, oral and intranasal administration of BSA loaded nanospheres. Vaccine. 2002; 21:67–77. [PubMed: 12443664]
26. Fahmy TM, Samstein RM, Harness CC, Saltzman WM. Surface modification of biodegradable polyesters with fatty acid conjugates for improved drug targeting. Biomaterials. 2005; 26:5727–36. [PubMed: 15878378]
27. Steenblock ER, Fahmy TM. A comprehensive platform for ex vivo T-cell expansion based on biodegradable polymeric artificial antigen-presenting cells. Mol Ther. 2008; 16:765–72. [PubMed: 18334990]
28. Clawson C, Huang CT, Futalan D, Seible M, Saenz R, Larsson M, et al. Delivery of a peptide via poly(d, l-lactic-co-glycolic) acid nanoparticles enhances its dendritic cell–stimulatory capacity. Nanomedicine. Oct; 2010 6(5):651–61. [PubMed: 20348031]
29. Win KY, Feng SS. Effects of particle size and surface coating on cellular uptake of polymeric nanoparticles for oral delivery of anticancer drugs. Biomaterials. 2005; 26:2713–22. [PubMed: 15585275]
30. Moore KJ, Khoury EJ, Medeiros LA, Terada K, Geula C, Luster AD, et al. CD36-initiated signaling cascade mediates inflammatory effects of beta-amyloid. J Biol Chem. 2002; 277:47373–9. [PubMed: 12239221]
31. Serghides L, Smith TG, Patel SN, Kain KC. CD36 and malaria: friends or foes? Trends Parasitol. 2003; 10:461–9. [PubMed: 14519584]
32. Shrimpton RE, Butler M, Morel AS, Eren E, Hue S, Ritter MA. CD205 (DEC-205): a recognition receptor for apoptotic and necrotic self. Mol Immunol. 2009; 46:1229–39. [PubMed: 19135256]
33. Chung EY, Liu J, Homma Y, Zhang Y, Brendolan A, Saggese M, et al. Interleukin-10 expression in macrophages during phagocytosis of apoptotic cells is mediated by homeodomain proteins Pbx1 and Prep-1. Immunity. 2007; 27:952–64. [PubMed: 18093541]
34. Sharp FA, Ruane D, Class B, Creagh E, Harris J, Malyala P, et al. Uptake of particulate vaccine adjuvants by dendritic cells activates the NALP3 inflammasome. Proc Natl Acad Sci USA. 2009; 106:870–5. [PubMed: 19139407]
35. Uto T, Wang X, SatoK, Haraguchi M, Akagi T, Akashi M, et al. Targeting of antigen to dendritic cells with poly(gamma-glutamic acid) nanoparticles induces antigen-specific humoral and cellular immunity. J Immunol. 2007; 178:2979–86. [PubMed: 17312143]
36. Heuking S, Adam-Malpel S, Sublet E, Iannitelli A, Stefano A, Borchard G. Stimulation of human macrophages (THP-1) using toll-like receptor-2 (TLR-2) agonist decorated nanocarriers. J Drug Target. 2009; 17:662–70. [PubMed: 19694614]
37. Hamdy S, Molavi O, Ma Z, Haddadi A, Alshamsan A, Gobti Z, et al. Co-delivery of cancer-associated antigen and Toll-like receptor 4 ligand in PLGA nano-particles induces potent CD8+ T cell-mediated anti-tumor immunity. Vaccine. 2008; 26:5046–57. [PubMed: 18680779]
38. Diwan M, Elamanchili P, Lane H, Gainer A, Samuel J. Biodegradable nanoparticle mediated antigen delivery to human cord blood derived dendritic cells for induction of primary T cell responses. J Drug Target. 2003; 11:495–507. [PubMed: 15203918]
39. Elamanchili P, Lutsiak CM, Hamdy S, Diwan M, Samuel J. “Pathogen-mimicking” nanoparticles for vaccine delivery to dendritic cells. J Immunother. 2007; 30:378–95. [PubMed: 17457213]
40. Borges O, Cordeiro-da-Silva A, Tavares J, Santarém N, de Sousa A, Borchard G, et al. Immune response by nasal delivery of hepatitis B surface antigen and codelivery of a CpG ODN in alginate coated chitosan nanoparticles. Eur J Pharm Biopharm. 2008; 69:405–16. [PubMed: 18364251]
41. Reddy ST, Swartz MA, Hubbell JA. Targeting dendritic cells with biomaterials: developing the next generation of vaccines. Trends Immunol. 2006; 27:573–9. [PubMed: 17049307]
42. Jones KS. Biomaterials as vaccine adjuvants. Biotechnol Prog. 2008; 24:807–14. [PubMed: 19194892]
43. Tacken PJ, Torensma R, Figdor CG. Targeting antigens to dendritic cells in vivo. Immunobiology. 2006; 21:599–608. [PubMed: 16920498]

44. Espuelas S, Thumann C, Heurtault B, Schuber F, Frisch B. Influence of ligand valency on the targeting of immature human dendritic cells by mannosylated liposomes. Bioconjug Chem. 2008; 19:2385–93. [PubMed: 19053315]
45. Mahnke K, Guo M, Lee S, Sepulveda H, Swain SL, Nussenzweig M, et al. The dendritic cell receptor for endocytosis, DEC-205, can recycle and enhance antigen presentation via major histocompatibility complex class II-positive lysosomal compartments. J Cell Biol. 2000; 151:673–84. [PubMed: 11062267]
46. Kwon YJ, James E, Shastri N, Fréchet JM. In vivo targeting of dendritic cells microparticles. Proc Natl Acad Sci USA. 2005; 102:18264–8. [PubMed: 16344458]
47. Chieppa M, Bianchi G, Doni A, Del Prete A, Sironi M, Laskarin G, et al. Cross-linking of the mannose receptor on monocyte-derived dendritic cells activates an anti-inflammatory immunosuppressive program. J Immunol. 2003; 171:4552–60. [PubMed: 14568928]
48. Puffer EB, Pontrello JK, Hollenbeck JJ, Kink JA, Kiessling LL. Activating B cell signaling with defined multivalent ligands. ACS Chem Biol. 2007; 2:252–62. [PubMed: 17432821]
49. Gestwicki JE, Cairo CW, Strong LE, Oetjen KA, Kiessling LL. Influencing receptor-ligand binding mechanisms with multivalent ligand architecture. J Am Chem Soc. 2002; 124:14922–33. [PubMed: 12475334]
50. Ullrich' A, Schlessingert J. Signal transduction by receptors with tyrosine kinase activity. Cell. 1990; 61:203–12. [PubMed: 2158859]
51. Silverstein RL, Febbraio M. CD36, a scavenger receptor involved in immunity, metabolism, angiogenesis, and behavior. Sci Signal. 2009; 2:1–8. [PubMed: 19318623]
52. Silverstein RL, Febbraio M. CD36 and atherosclerosis. Curr Opin Lipidol. 2000; 11:483–91. [PubMed: 11048891]
53. Kunjathoor VV, Febbraio M, Podrez EA, Moore KJ, Andersson L, Koehn S, et al. Scavenger receptors class A-I/II and CD36 are the principal receptors responsible for the uptake of modified low density lipoprotein leading to lipid loading in macrophages. J Biol Chem. 2002; 277:47373–9. [PubMed: 12239221]
54. Tagliani E, Guermonprez P, Sepúlveda J, López-Bravo M, Ardavín C, Amigorena S, et al. Selection of an antibody library identifies a pathway to induce immunity by targeting CD36 on steady-state CD8 alpha+ dendritic cells. J Immunol. 2008; 180:3201–9. [PubMed: 18292544]
55. Inaba K, Inaba M, Romani N, Aya H, Deguchi M, Ikehara S, et al. Generation of large numbers of dendritic cells from mouse bone marrow cultures supplemented with granulocyte/macrophage colony-stimulating factor. J Exp Med. 1992; 176:61693–702.

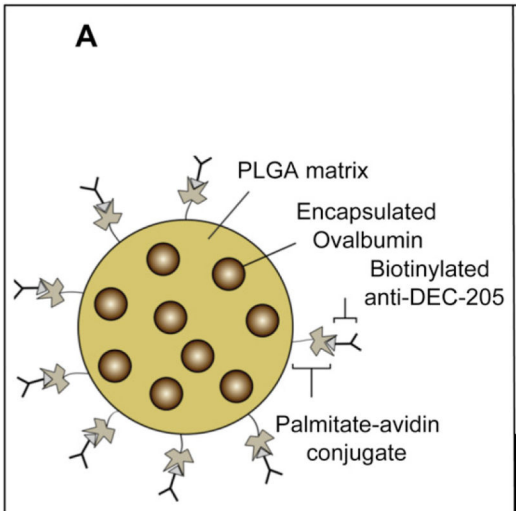

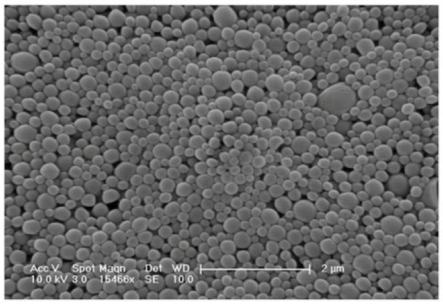

C	Surface Modification of Particle	Average Diameter	Poly dispersity
None		210±2.5nm	0.195
5 μg anti-DEC 205 mAb/mg nanoparticle		225±4.6nm	0.185
25 μg anti-DEC 205 mAb/mg nanoparticle		245±3.8nm	0.178

Fig. 1.

Description of nanoparticles. (A) Schematic representation of nanoparticles surface modified with avidin to facilitate binding of a biotinylated ligand (not to scale). (B) Scanning electron microscopy image of surface modified nanoparticles. (C) Measurement of size and polydispersity of unmodified and surface modified nanoparticles by dynamic light scattering.

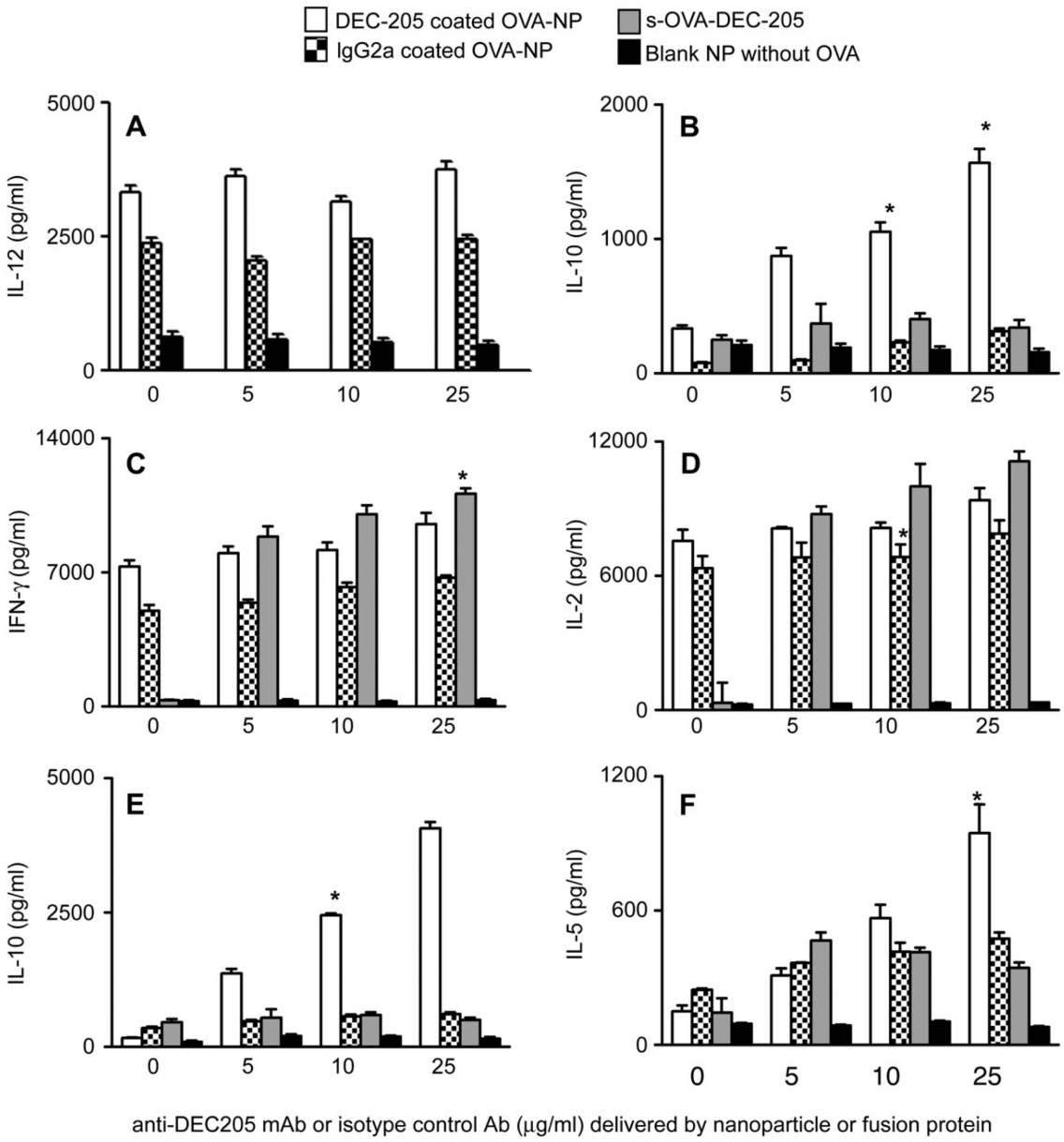

Fig. 2.

Targeted nanoparticles induce DC production of cytokines that promote Th1 and Th2 cell cytokine production. DCs were incubated with the indicated nanoparticles or s-Ova-DEC-205 conjugate for 8 h, after which uningested stimuli were removed. DCs were incubated with fresh media for another 24 h (Panels A, B), or with OTII T cells in fresh media for 72 h (Panels C–F). Cytokines were measured by cytokine-specific ELISA at the end of the incubation periods. Values on the x-axis represent the amount of anti-DEC-205 mAb or isotype control mAb (IgG2a) in the nanoparticle or s-Ova-DEC-205 preparation. Results were expressed as the amount of indicated cytokine (pg/ml) ± SE. Experiments were done independently at least three different times and statistical analysis was performed using the Student *t* test between the control groups and the experimental groups (*$p < 0.05$).

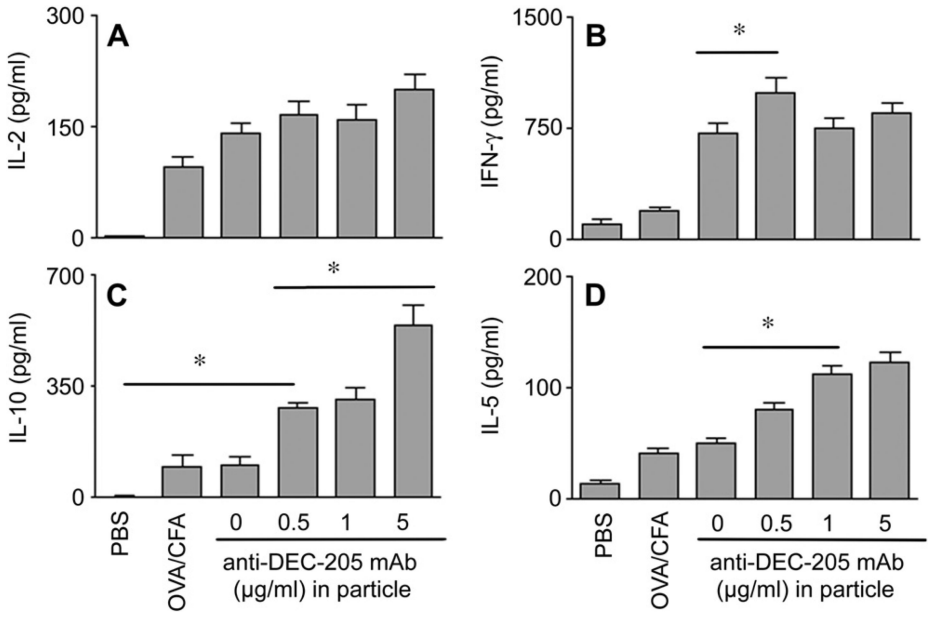

Fig. 3.

Secondary immunization of mice primed with OVA in CFA broadens the T cell cytokine response. Groups of 4 mice were immunized by i.p. injection of 100 μg OVA emulsified in CFA or sham immunized with PBS. One wk later, groups of mice were boosted by i.p injection of 2 mg of the non-targeted or targeted OVA-nanoparticles, the latter surface modified with the indicated amount of anti-DEC-205 mAb. Cytokine production by whole splenocytes restimulated with OVA was assessed by cytokine-specific ELISA 1 wk after secondary immunization. The experiment was performed 2 times and results are expressed as mean ± SE. Statistical significance was determined using the Student *t* test (*$p < 0.05$).

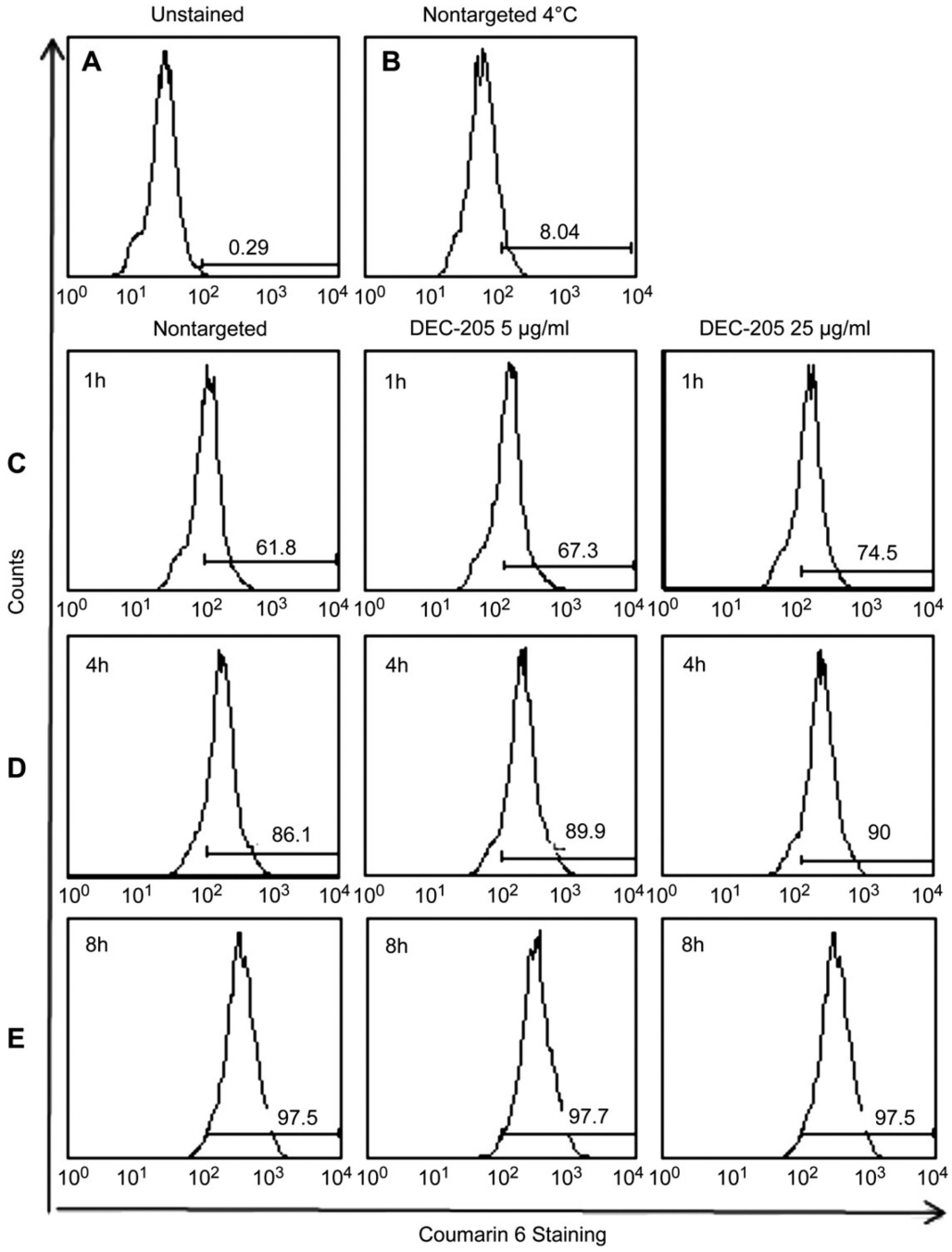

Fig. 4.

Flow cytometry assessment of DC internalization of non-targeted versus targeted nanoparticles. DCs were exposed for 1, 4 or 8 h to Coumarin-6 containing nanoparticles with or without surface modification with 5 or 25 μg anti-DEC-205 mAb per mg particles. After the indicated times, the cells were stained with CD11c-APC and fixed. Histograms depict Coumarin-6 fluorescence intensity for the gated CD11c+ population. A) CD11c+ cells without exposure to Coumarin-6 containing nanoparticles; B) cells exposed to non-

targeted nanoparticles held at 4 °C for 8 h; C–E) Cells exposed to the indicated nanoparticles for 1 h (Panel C), 4 h (Panel D) or 8 h (Panel E). MFI values are reported in Table 1.

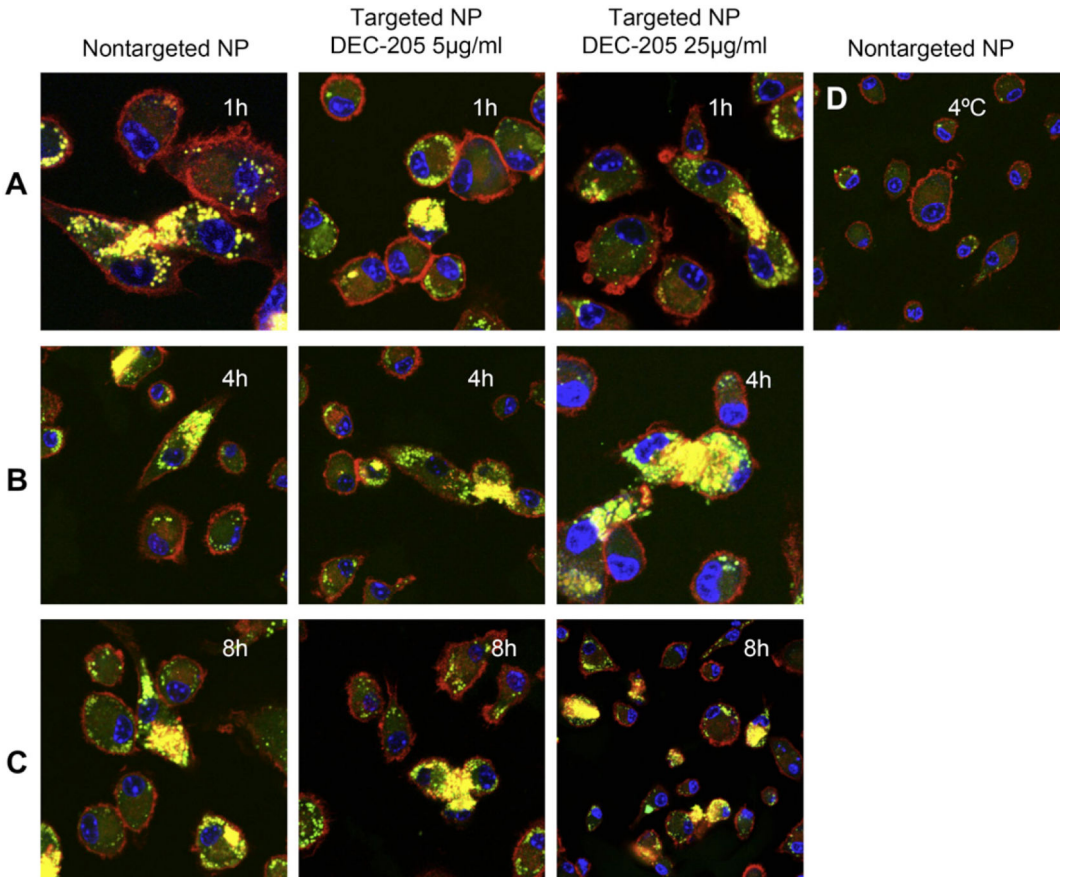

Fig. 5.

Confocal imaging analysis of DC uptake of targeted versus non-targeted nanoparticles. DCs were plated onto alcian blue coated cover slips, then exposed for 1, 4 or 8 h to Coumarin-6 containing nanoparticles with or without surface modification with anti-DEC-205 mAb (5 or 25 μg/mg particles). After the indicated times, cells were fixed and stained with Alexa Fluor® 548 phalloidin to label F-actin (red) and ToPro-3 to label the nucleus (blue). Cells were visualized under Zeiss confocal microscope using wavelengths 488, 568 and 633 nm. The microscope used is a Zeiss LSM510Meta, configured on an inverted Axio200M microscope with 10x-NA 0.30, 25XW-NA 0.80, and 63WX-NA1.2 lenses. Software and detection system are inclusive to the microscope.

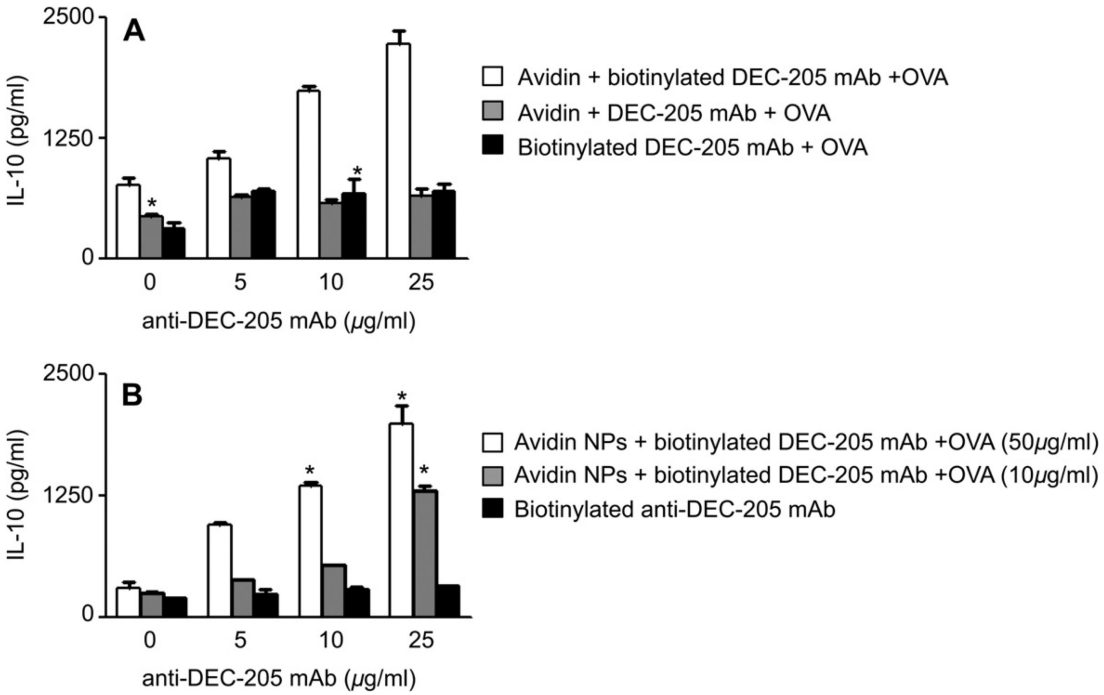

Fig. 6.

Multivalent preparations of anti-DEC-205 mAb are required for IL-10 production. DCs were incubated with multimers of avidin and biotin anti-DEC-205 in concentrations similar to present on nanoparticle surface. As controls, DCs were also incubated with avidin and anti-DEC-205 and biotin anti-DEC-205 mAb for 4 h. Soluble OVA was added to each sample at a concentration of 50 μg/ml. In another treatment group, DCs were incubated with nanoparticles not encapsulating OVA but surface modified with avidin. These particles were surface modified with biotin anti-DEC-205 (25, 10 and 5 and 0 μg/ml) and soluble OVA were added to each sample in two different concentrations (50 and 10 μg/ml). As a control DCs were incubated with particles containing OVA but not surface modified with avidin and biotin anti-DEC-205 was added to each sample in different concentrations. After 4 h of incubation, uningested particles and complexes were washed off and purified naïve OTII Tg T cells were added and incubated for 72 h. Supernatants were harvested and assayed for IL-10 using cytokine-specific ELISA (BD Pharmingen). Experiments were repeated at least twice and statistical differences between the control groups and the experimental groups was determined using the Student *t* test (*$p < 0.05$).

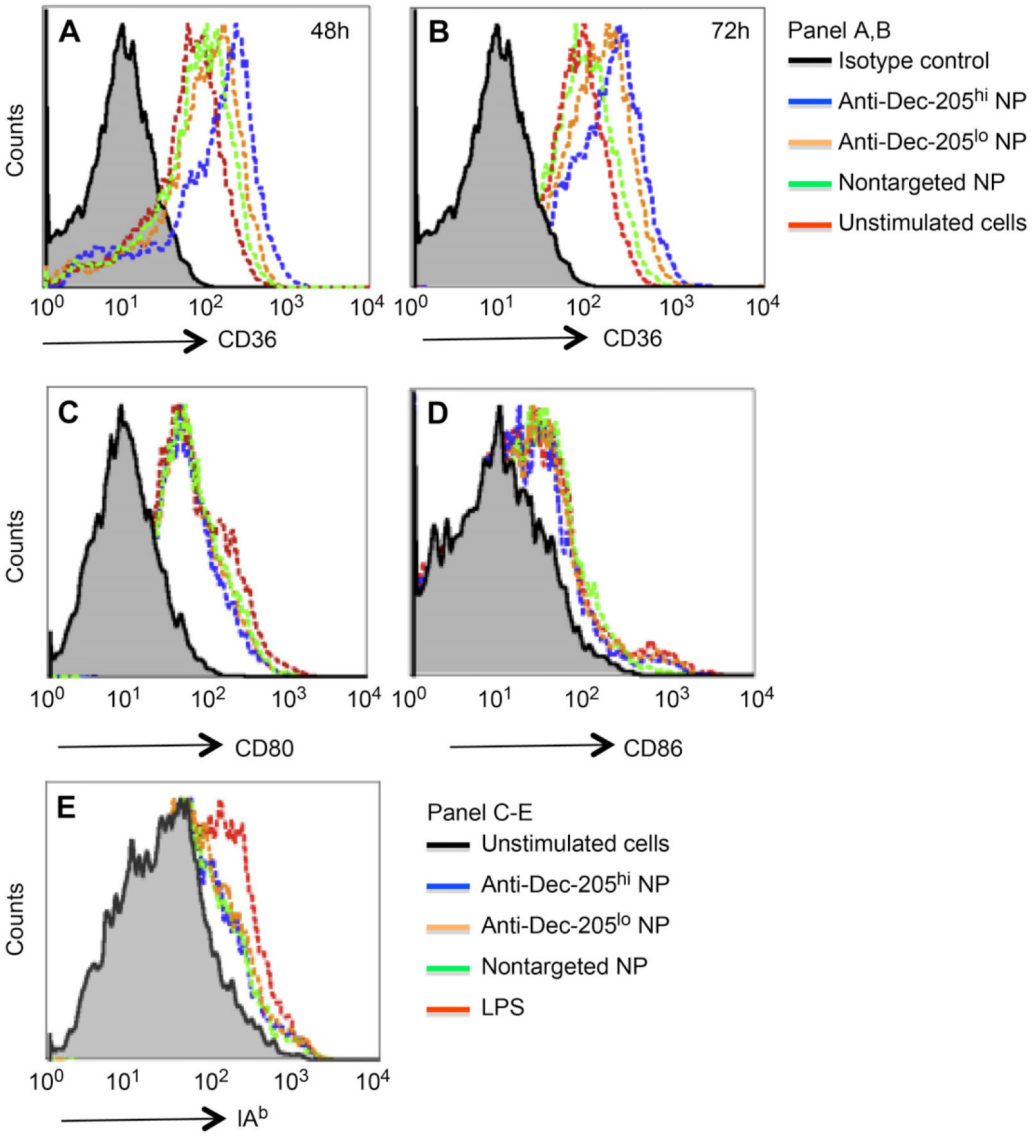

Fig. 7.

DEC-205 targeted nanoparticles upregulate CD36 expression on DCs. DCs were incubated with non-targeted or targeted nanoparticles modified with the low (5 μg/mg nanoparticle) or high (25 μg/mg nanoparticle) anti-DEC-205 mAb. After 4 h, the stimuli were removed and fresh media added. Changes in expression of CD36 were measured by flow cytometry at 48 h (Panel A) and 72 h (Panel B), and compared with changes in expression of expression of the T cell costimulatory molecules CD80 (Panel C) and CD86 (Panel D) or IA^b (Panel E) at 24 hrs.

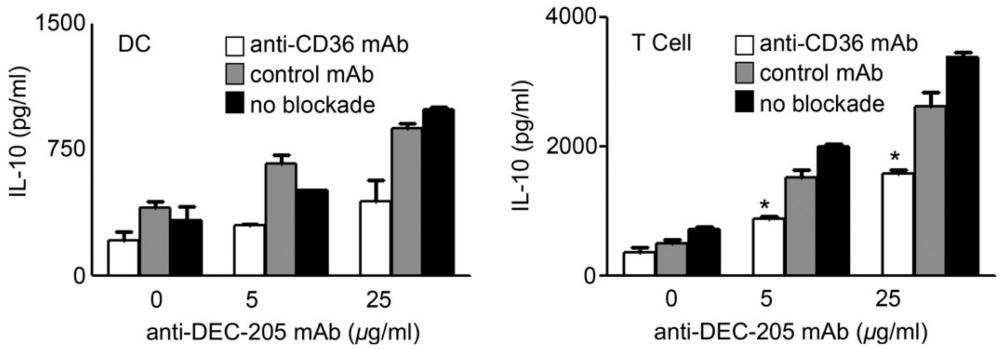

Fig. 8.

Blockade of CD36 reduces DC production of IL-10 after exposure to targeted nanoparticles. DCs were incubated with the CD36 blocking mAb (FA6152, Abcam), an isotype control mAb or media only for 30 min prior to exposure to non-targeted or targeted nanoparticles. After 4 h exposure, particles were washed away and OTII T cells added in fresh media containing antibody to CD36, isotype control or no antibody. After 72 h, cytokines in cell free culture supernatants were measured by cytokine-specific ELISA. CD36 –/– animals were also used for the same study and compared the responses to the wild type animal. Experiments were done independently at least three different times and statistical differences between the control groups and the experimental groups were determined using the Student *t* test (*$p < 0.05$).

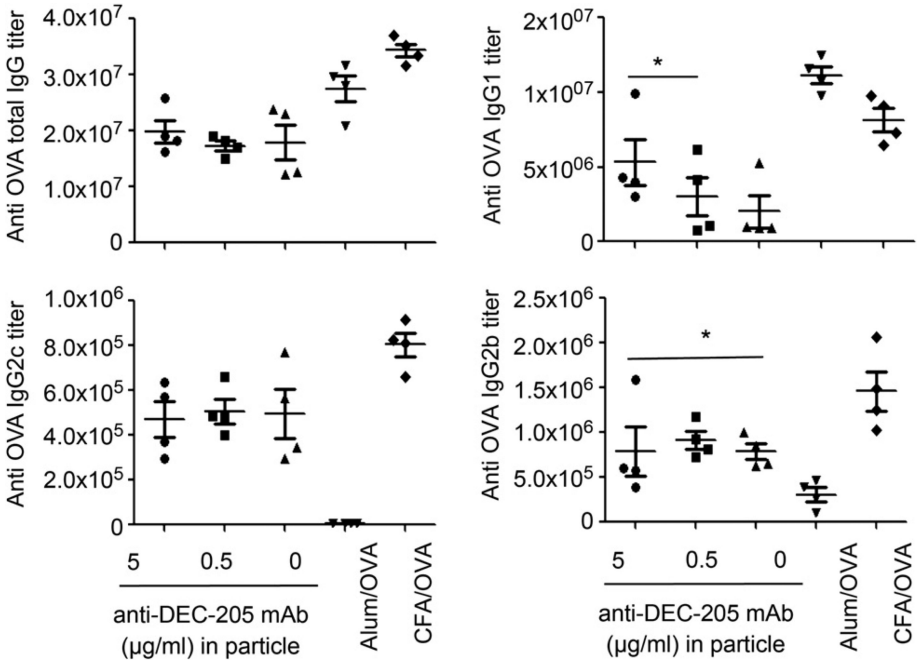

Fig. 9.

Groups of four mice were immunized by i.p. injection in 300 μl PBS containing 2 mg OVA-nanoparticles (30 μg OVA) surface modified with 0, 0.5 or 5 μg/ml anti-DEC-205 mAb. As positive controls, mice were primed with similar concentrations of OVA (30 μg) in CFA and OVA (30 μg) in Allhydrogel. Serum isolated at week 2 and analyzed for OVA specific titers of total IgG, IgG1, IgG2b, and IgG2c by ELISA. Blank nanoparticles containing no OVA were used as the negative controls. Experiments were repeated two times and the statistical differences between controls and experimental groups were determined using Student *t* test.

Table 1

Induction of CD36 expression by non-targeted versus targeted nanoparticles in comparison to s-OVA-DEC-205.

Stimulus	MFI (24 h)	MFI (48 h)	MFI (72 h)
Control mAb	9.3 ± 0.9	8.6 ± 1.9	10.3 ± 2.1
Non-targeted NP	74.9 ± 1.4	105.4 ± 3.1	104.8 ± 1.5
Anti-DEC-205 mAb^{lo} NP	88.9 ± 0.5	119.0 ± 2.3	117.0 ± 1.8
Anti-DEC-205 mAb^{hi} NP	101.2 ± 2.2	160.0 ± 1.6	145.0 ± 0.8
No stimulus	65.5 ± 2.1	87.0 ± 1.4	94.0 ± 2.0
s-Ova-DEC-205	72.5 ± 1.4	99.0 ± 2.2	99.2 ± 2.6